

OMAE2008-57648

CHARACTERISTICS OF THE INFRAGRAVITY WAVE CLIMATE

Stephen Masterton

Shell International
Exploration & Production B.V.
Kessler Park 1, Rijswijk 2288 GS,
The Netherlands
Email: stephen.masterton@shell.com

Kevin Ewans

Shell International
Exploration & Production B.V.
Kessler Park 1, Rijswijk 2288 GS,
The Netherlands
Email: kevin.ewans@shell.com

ABSTRACT

Infragravity waves are very long period waves below the frequency of typical wind waves. They are most significant in shallow water locations and therefore have a high impact on the response of moored vessels. For the Oil and Gas business this can be an important consideration for tanker on/offloading operations (including LNG vessels) - these larger vessels, with longer natural periods, are particularly susceptible. There are implications for both the design and operation including the calculation of extreme loading on the mooring system, extreme vessel motions, fatigue of mooring systems and the availability of on/offloading operations.

There are currently limited design practices to account for the effect of infragravity waves. This may be attributed to two main factors: The development of infragravity waves is difficult to model and is sensitive to many factors, including the magnitude and shape of the incident wind and swell spectra, local bathymetry, directionality and near shore wave breaking. Secondly, very little measured data exist since the infragravity wave frequencies lie below the conventional range of commonly deployed wave measurement devices.

The present paper will provide a description of the infragravity waves acting on the US coast at two locations, Duck, North Carolina, and Baja, California. The results will characterize parameters including the significant wave height, peak period, and comparison of infragravity waves through time. In addition, the relationships between the spectral shape will be examined including directionality. This type of information is needed to set design criteria for infragravity waves, and in the longer

term to develop and enhance infragravity wave models e.g. Reniers 2002 (1) and ultimately contribute to establishing design practices.

1 Introduction

Infragravity waves represent an important consideration for the design and operation of coastal infrastructure for the oil and gas industry. Infragravity waves are long period oscillations (approximately 20-300 sec) arising well below the frequency of typical wind and swell waves. Although the wave height of the infragravity motion is small compared to wind and swell, their long wave period may excite large resonant motions of floating structures, particularly large vessels. The immediate practical considerations are therefore mooring system design and vessel motion, including extremes and perhaps more significantly on/offloading operability. With the current industry trends towards larger and larger vessels and consideration of other (large) floating concepts it is anticipated that this subject area will be of growing importance. Presently, this problem is the subject of much collaborative research to better understand vessel dynamics in shallow water. This paper will discuss the characteristics of the infragravity wave climate using data from two different locations. Aspects including the distribution of wave height and the relationship between the short wave climate (wind and swell waves) and the infragravity wave climate will also be considered.

2 Measured Data and Processing

Two data sets are investigated in the present paper. The first is for the Duck location on the US East Coast, North Carolina. The data were provided and obtained by the Field Research Facility of the US ARMY corps of engineers. This data set covers the complete year of 2005 and includes waverider buoy data and pressure measurements from a 15 gauge pressure transducer array. Raw time series data were provided with minimal quality control (QC) applied, all the QC routines would be developed as part of the present analysis to ensure compatibility with infragravity wave analysis.

For the present analysis the pressure transducer data were used to extract the infragravity wave spectra. The data from the waverider buoy were also processed but only used to check the short wave spectra derived from the pressure transducer array. This is because the conventional waverider buoy is unable to resolve frequencies down to the infragravity range. The pressure gauge array is located in approximately 8m water depth and consists of 15 gauges arranged in a cross configuration. This is orientated in both alongshore and crossshore directions. For more details of this facility the reader is referred to the Field Research facility website and (for example), papers by (2; 3). Raw data were provided at 2Hz in continuous sections of approximately 2 hours 50 minutes (20480 points) every 3 hours.

The data for the Baja location was obtained using a GPS waverider buoy sampled continuously at 2Hz. The GPS waverider buoy measures the x , y , z velocities rather than accelerations, as per conventional wavebuoys (for example, the waverider deployed at the Duck location). Since the position is derived from a single integration it is possible for a GPS waverider to measure frequencies down to approximately 100 seconds, (4) therefore estimates of infragravity waves may be acquired.

In order to resolve the infragravity waves and maintain a sufficient number of averages per frequency bin a subseries of 2048 points was chosen. This allowed 19 averages with half overlapping applied to the full record of 20480 points. Adopting this method the resolution in frequency, Δf was approximately 0.001 Hz (1/1024). Infragravity response was considered to lie nominally within the range $4-52 \Delta f$ or waves with period $340 - 19.7s$. For the analysis of the Baja data, (the second dataset considered in the present paper) a narrower limit was adopted. This is described later in the text.

As a final note the infragravity wave spectra in the present study are omni-directional and represent only the total energy without consideration or distinction between wave components that are bound and those that are free. Addressing the latter aspect is currently the focus of ongoing work, in addition to a directional analysis of infragravity waves. The short wave directional spectra have been calculated using standard techniques and corresponding parameters including H_s , T_p , and peak direction to investigate any correlation between the short wave and the infragravity wave climate.

3 Discussion

Figure 1 provides a timeseries of H_s (defined as $4\sqrt{m_0}$) at the Duck location. The figure covers the complete year over three subplots (a) – (c); (a) shows the data for January to April, (b) May - August and (c) September to December approximately. The blue line represents the H_s calculated from the present analysis, as an independent check this was compared against the H_s published on the FRF website and is plotted in green. As should be

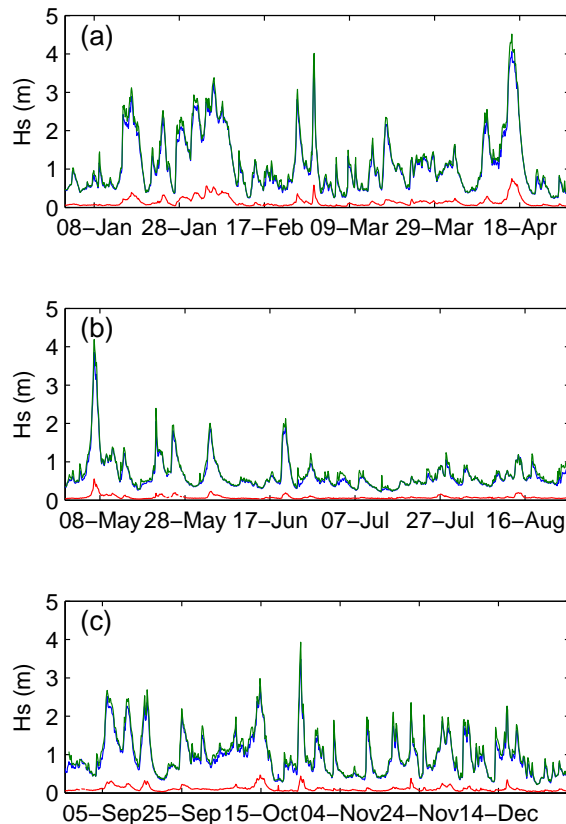


Figure 1: Timeseries of total H_s and H_s Infragravity, — H_s total from present analysis, — H_s total from FRF website for comparison, — H_{sIGtot} total infragravity significant waveheight

expected the lines are in good agreement, confirming the analysis is consistent. In addition, other parameters were checked, including directional parameters, equally good agreement was observed. The total infragravity significant waveheight (H_{sIGtot}) is also shown in Fig. 1 as the red line. It is most obvious that the waveheight of the infragravity waves is significantly smaller than for the short waves, in this data set the average (H_{sIGtot}) is 0.11m with maximum of 0.75m. However, the 'smaller' wave height by comparison to wind and swell is by no means an indication of

the design significance, since structural responses at infragravity wave periods are markedly different. Figure 1 shows that the significant waveheight of the infragravity waves appears to be correlated to the short wave H_s . Closer inspection of the data also highlights some areas of high infragravity wave activity but arising with a relatively low magnitude of short wave H_s . This will be investigated further using scatter plots of H_s and $H_{SI_{Gtot}}$ but first we consider the annual distribution of infragravity waveheight and extreme value analysis.

Figure 2 demonstrates the distribution of infragravity waveheight for the full year of data. A histogram is shown in subplot (a) for the 2893 observations of infragravity significant waveheight. This plot illustrates the skew in the data towards the ambient, low values of infragravity waves and is reflected in the cumulative probability curve shown in subplot (b). This probability density function is calculated using a kernel density estimator method. The mean, median and mode are respectively: 0.11m, 0.076m and 0.029m. To model the distribution of $H_{SI_{Gtot}}$

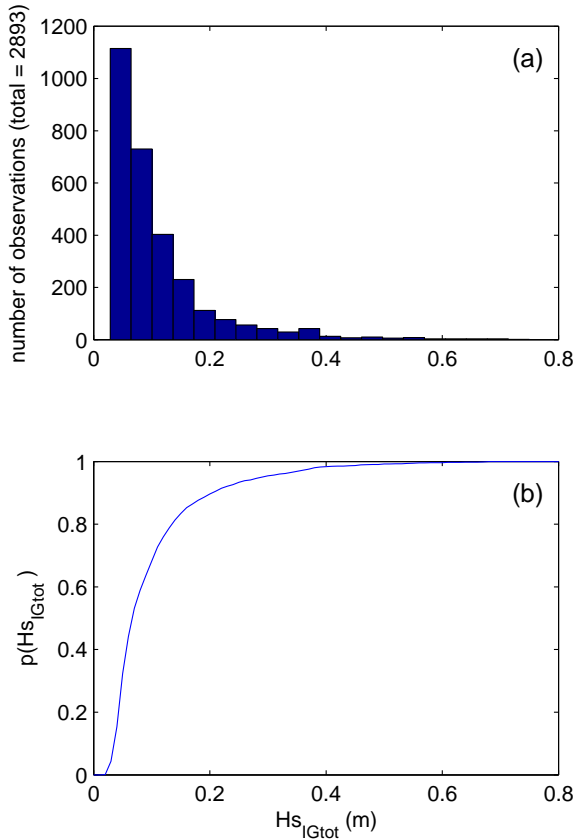


Figure 2: Distribution of total infragravity significant waveheight $H_{SI_{Gtot}}$ for one year of observations at the Duck location (a) histogram of $H_{SI_{Gtot}}$; (b) cumulative distribution function

and to obtain some estimates of the independent extreme values, an extreme value analysis (EVA) was performed on the dataset. This analysis was carried out using the Shell Metocean group in-house EVA tools using standard techniques. A fit was achieved using a Weibull distribution with a truncated dataset. The latter was employed since the population of extremes was deemed to be different to the ambient infragravity wave climate. Figure 3 provides a non-exceedence plot of the data and a best fit Weibull curve. The plot also shows the 5–95% confidence interval which captures all the data points. Summary tables are also included providing the $H_{SI_{Gtot}}$ values for return periods of 1 month, 1, 2, and 10 years. It should be noted that these estimates are preliminary and should not be used for design.

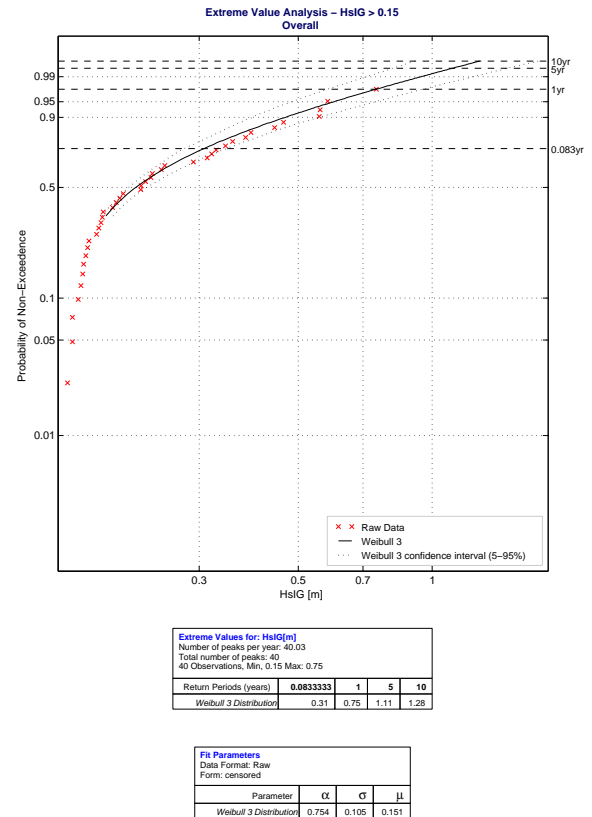


Figure 3: Preliminary extreme value analysis of $H_{SI_{Gtot}}$ fitting a Weibull distribution to one year of observations at the Duck location. NOT TO BE USED FOR DESIGN

Previous discussion has concentrated on the distribution of infragravity waveheight. The following discussion will consider the relationship between infragravity waves and the corresponding short wave spectrum. This aspect is of importance since the identification of any correlation will facilitate the development

of infragravity wave models. For engineering design infragravity wave modelling becomes essential because large datasets of low frequency waves are simply not available. Infragravity waves must be estimated based on measured or hindcast short wave data. Indeed, while previous studies show some correlation between the infragravity waves and their associated short waves, the relationship is far from simple. Models must account for, amongst others, the physical processes of wave – wave interaction, interaction with bathymetry, and wave breaking. As part of the ongoing work a collaborative validation study of the model by (1) is in progress (the early stages of this work is described in (5)). The following paragraphs confirm some of the previously identified relationships existing in the data.

Figure 4 shows a scatter plot of H_s vs. H_{SIGtot} for all 2893 observations in the full year of Duck data. There is a very clear and positive correlation in the data. The shape of the scatter curve suggests a steepening gradient as the H_s becomes larger. However, without further data there is little justification to fit anything other than a straight line. We also comment that a best fit curve does not necessarily lie on the origin (0,0) since the presence of ambient infragravity waves with no correlation to the short wave H_s is also a realistic scenario.

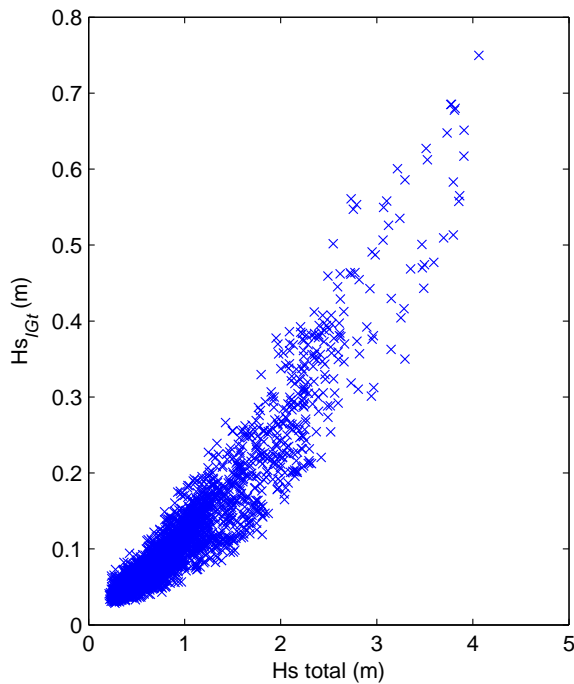


Figure 4: Scatter plot of total H_s vs H_s Infragravity for one year of observations at the Duck location

Generally accepted theory into the cause of infragravity

waves states that the observed infragravity waves are dominated by two effects, the first, from the (predictable) second order difference waves bound to the incoming short wave system, while the second, are free infragravity waves propagating away from the beach. The latter are generated through breaking of the incident short waves and subsequent 'release' and reflection of the bound infragravity wave components. These difference terms are strongly related to the spectral shape, where narrow banded long crested wave spectra generate a larger magnitude of difference response.

Figure 5 shows a scatter plot of H_{SIGtot} vs. the directional spread of the peak frequency for the short wave spectrum. The larger the directional spread (the x axis) the more short crested the sea state, and associated reduction in (theoretical) second order difference terms. The graph shows that there is a mean di-

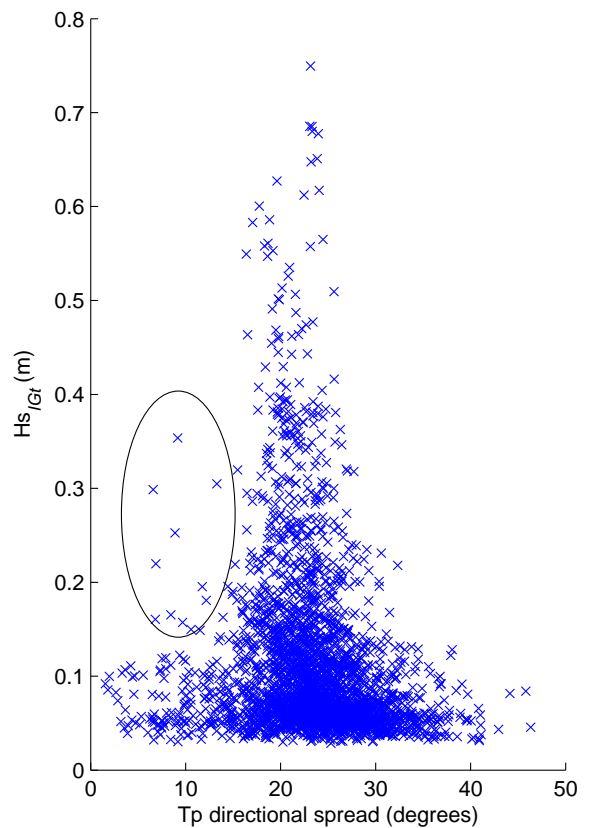


Figure 5: Scatter plot of short wave directional spread vs. H_{SIGtot} total infragravity significant waveheight for one year of observations at the Duck location

rectional spread (between 20 and 30 degrees) that the majority of all observations lie within. i.e. this band has the highest density of points. This distribution would be entirely expected in the

absence of any relationship between spreading and infragravity wave height. However, there are a number of observations circled in the diagram that show abnormally large infragravity responses at very low values of directional spread (long crested waves). Since we have seen a good correlation between H_s and H_{SIGtot} Figure 4 with no such outliers we may conclude that the presence of small directional spread has contributed the infragravity response.

Figure 6 shows a polar plot of the infragravity wave height compared with the direction of the incident short wave system. There are two subplots, the first shows the mean wave direction at the spectral peak and the second shows additionally the main wave direction. The directions are expressed with the waves defined as arriving *from* the specified direction, where 0° is orientated such that it represents waves arriving normal to the direction of the coastline. Both plots demonstrate that the largest infragravity response is observed with incident wave direction at approximately -10° , and is consistent with the local short wave climate. It is also notable that a cloud of points (similar to those circled in Fig. 5) arising between -25° and -30° result in slightly larger than normal H_{SIGtot} .

Finally, the spectral shape of the infragravity waves at the Duck location has been investigated. This was first achieved by analysing the location of the spectral peak within the infragravity range. Figure 6 shows a scatter plot of the peak period vs significant waveheight of the infragravity waves. The peak periods plotted along the x axis are specified in discrete bins and are non uniformly spaced since each bin represents the reciprocal of uniformly spaced frequency bins. The plot indicates that the peak is typically between 100 seconds and that significant energy is also present up to periods between 200 and 300 seconds.

Figure 8 shows the average shape of selected infragravity spectra at the Duck location. These have all been normalised by the total infragravity variance. The average of these normalised spectra has been overlaid in bold. Clearly, there is a characteristic spectral shape associated with the observations at this location. Furthermore, it is interesting to note that there is an apparent oscillation in these spectra. Further investigation has confirmed the existence of this oscillation across a number of independent pressure transducers. As yet, the authors are unable to propose a firm explanation for these observations.

The following discussion concerns the analysis of data from the Baja location. The discussion will follow broadly that provided for the Duck location, namely, a timeseries analysis of the infragravity significant waveheight H_s , its statistical distribution, the correlation with the short wave significant waveheight and finally an examination of the spectral shape. There are two notable differences between the Baja and the Duck data. the first is simply the location, but the second is due to the instrument used for measurement. Following the Duck analysis, significant energy may be expected down to periods between 200–300 seconds. The latter aspect is significant for the interpretation of the

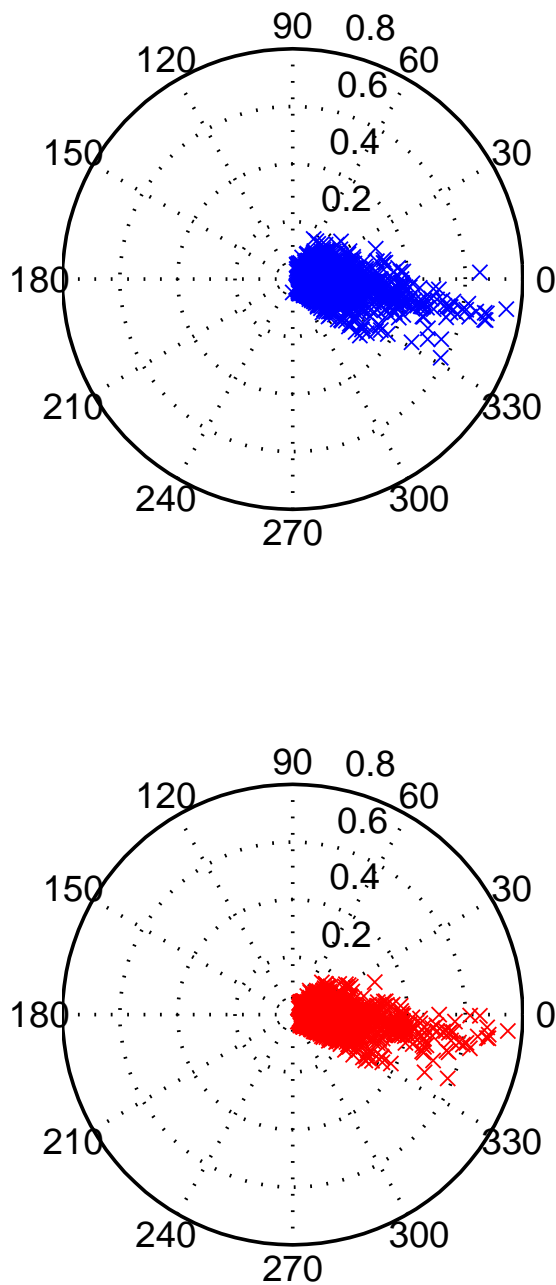


Figure 6: Polar plot of wave direction (direction from) and H_s Infragravity for one year of observations at the Duck location: (a) Mean wave direction at the spectral peak; (b) Main wave direction

Baja data because the GPS waverider is theoretically limited to periods in the order of 100 seconds. This aspect is discussed later when the spectral shape is considered.

Figure 9 plots a timeseries of significant wave height for the

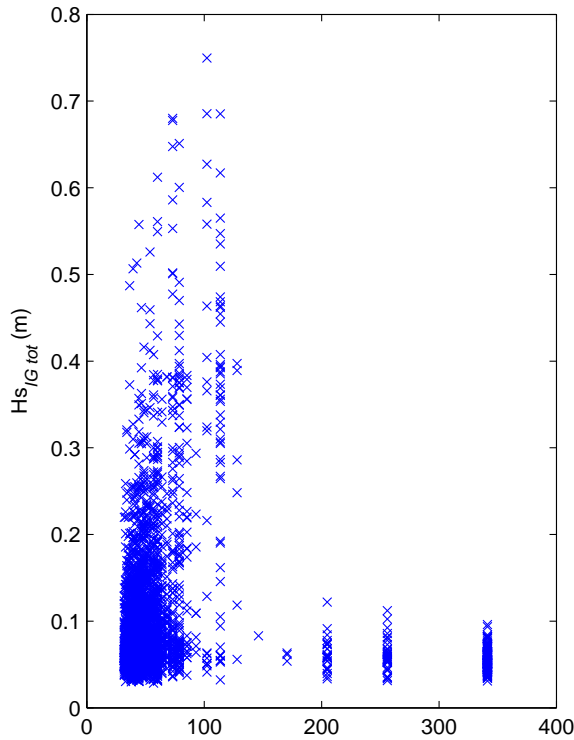


Figure 7: Scatter plot of Tp_{IG} Peak period of infragravity waves vs. significant waveheight for one year of observations at the Duck location: (a) Tp_{IG} vs. Hs Infragravity; (b) Tp_{IG} vs. Hs total

Baja location. Two lines have been included, the first for the total short wave Hs and the second for the infragravity wave Hs_{IGtot} . As an independent check the short wave Hs was compared with a nearby ADCP working in wave mode. Good agreement was found between data from these two instruments. In comparison to the Duck timeseries (Figure 1) there again appears to be a correlation between the infragravity Hs and the short wave Hs . However, the wave heights observed in the Baja data are significantly less than for Duck, the maximum Hs approximately 2.5m compared with approximately 4.5m at Duck. Interestingly, the ratios of infragravity wave height to total short wave height are less for the Baja location.

In Fig. 10 the distribution of infragravity significant waveheight is plotted. A histogram is shown in subplot (b). The skew in the data is similar to that exhibited in the Duck data however there are many observations with close to zero Hs_{IGtot} . The corresponding probability density function is shown in subplot (b).

Figure 11 shows a scatter plot of total Hs vs Hs_{IGtot} for the Baja location. the plot demonstrates that there is a good correlation between the magnitude of the short wave Hs and Hs_{IGtot} . However, it is apparent that the proportion of infragravity wave energy observed at the Baja location is somewhat lower in com-

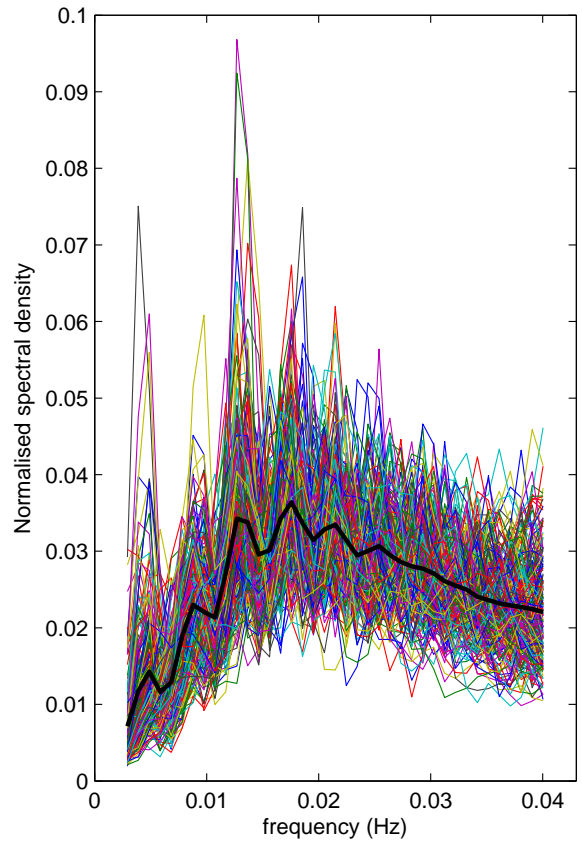


Figure 8: Infragravity wave spectral shape normalised by S_{η}/m_{0IG} where m_{0IG} is the variance of the infragravity band. The average is indicated by the solid black line

parison to that observed at Duck.

The spectral shape of the infragravity waves observed at the Baja location was considered. Figure 12 (a) provides a log plot of the spectral density for all observations. The frequency axis along the bottom is scaled from 0 to 0.3 Hz to capture the shape of the short wave spectrum. In part (b) the same data has been plotted but with the frequency scale zoomed in between 0 to 0.03Hz indicating the infragravity range. Clearly, there is an unsatisfactory roll off in the response of the GPS waverider buoy below about 0.01Hz. This is in agreement with the maximum resolution quoted in the literature (4). Given the previous results from Duck location indicating that significant energy may arise between 100 and 300 seconds we must note this shortcoming when interpreting these data. Notwithstanding, a clear spectral shape is apparent with the infragravity wave energy demonstrating a correlation to the short wave spectrum. Further work using additional data available for the Baja location will include the analysis of infragravity frequency data from the ADCP operating in wave mode.

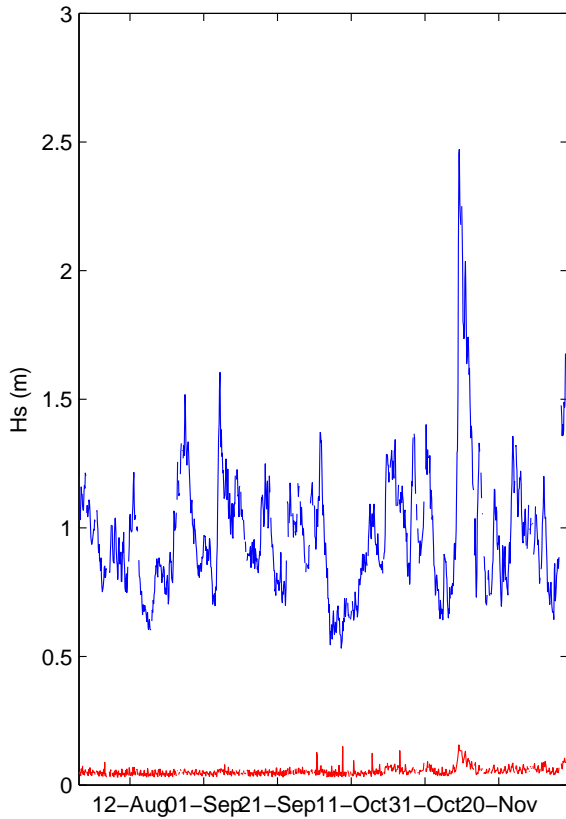


Figure 9: Timeseries of total H_s and H_s Infragravity for the Baja location: — H_s total from the present analysis, — H_{sIGtot} total infragravity significant waveheight

4 Conclusions and further work

The present paper has discussed aspects of the infragravity wave climate arising at two different locations; Duck, North Carolina and Baja on the US West Coast. For the former location the data covered the complete year of 2005. Raw pressure wave data have been analysed and the total infragravity wave spectra have been isolated. The data show that infragravity waves may arise with a significant wave height of up to 0.75m. The infragravity wave height has been shown to be strongly correlated with the significant waveheight of the underlying short wave system. Although this relationship shows a strong correlation there are clearly other dependencies such as the degree of directional spreading and the mean wave direction. In addition, the spectral shape of the infragravity waves were also investigated which demonstrated that significant infragravity energy is present down to wave periods between 100 and 300 seconds. It was noted that a clear spectral shape is associated with the occurrence of high infragravity wave activity.

These observations were also borne out through the analysis

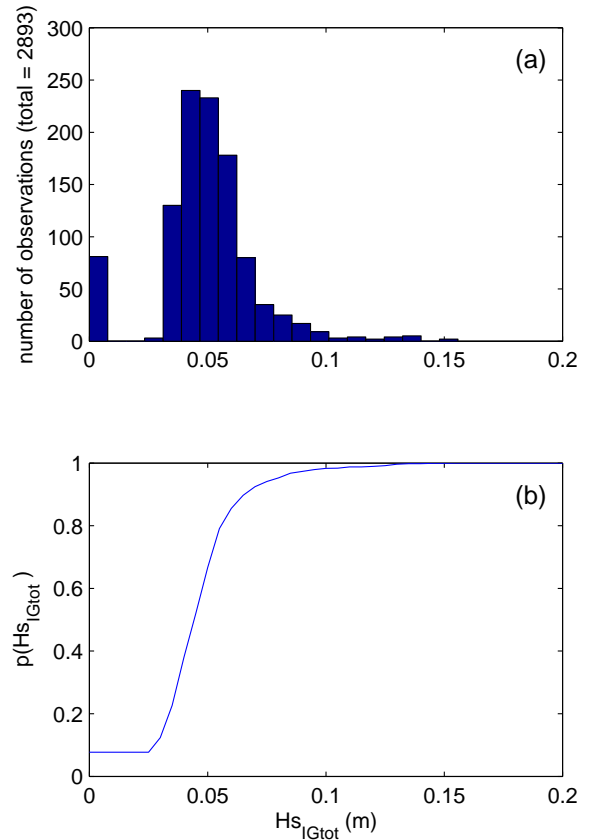


Figure 10: Distribution of total infragravity significant wave-height H_{sIGtot} for Baja location (a) histogram of H_{sIGtot} ; (b) cumulative distribution function

of data for the Baja location. Although the the findings were partially limited due to the lack of resolution for wave periods above 100 seconds. In conjunction with the Duck results there is strong evidence to suggest that infragravity wave activity has a distinct spectral shape and is highly correlated to the incident short wave spectrum.

The analysis of both data sets is presently ongoing and in parallel with an investigation of the Surfbeat infragravity wave model (1) (5). The ongoing work also includes a bi-spectral analysis of the wave data (not reported here) to separate the bound infragravity wave components from the free waves. In the longer term it is hoped that this studies such as this will contribute to the understanding of infragravity wave climatology and the refinement of predictive models. Ultimately leading to the establishment of suitable design practices to account for this still challenging phenomena.

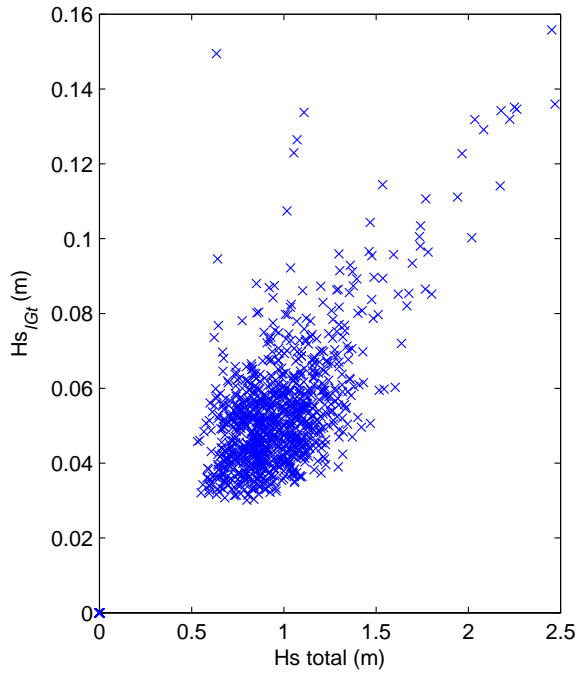


Figure 11: Scatter plot of total H_s vs H_s Infragravity for the Baja location

5 Acknowledgements

The authors wish to thank Charles Long of the Duck Field Research Facility and Ewoud van Haaften of Shell Global Solutions for the raw wave data. This work was undertaken partly through the SAFEOFFLOAD EU project.

REFERENCES

- [1] Reniers, A. J. H. M., van Dongeren, A. R., Battjes, J. A., and Thornton, E. B., 2002. "Linear modeling of infragravity waves during delilah". *Journal of Geophysical Research*, **107**, pp. 1–17. [1](#), [4](#), [7](#)
- [2] Herbers, T., Elgar, S., and Guza, R. T., 1995. "Infragravity-frequency (0.005-0.05hz) motions on the shelf. part ii: Forced waves". *Journal of Physical Oceanography*, **25**, pp. 1063–1079. [2](#)
- [3] Herbers, T., Elgar, S., and Guza, R. T., 1994. "Infragravity-frequency (0.005-0.05hz) motions on the shelf. part i: forced waves". *Journal of Physical Oceanography*, **24**, pp. 917–927. [2](#)
- [4] Jeans, G., and Feld, G., 2003. "The measurement and analysis of long period waves to support coastal engineering". In 30th IAHR Congress long period waves symposium Thessaloniki Greece 24–29 April, vol. 175, pp. 409–421. [2](#), [6](#)
- [5] Groenewegen, M. J., Reniers, A. J. H. M., Ewans, K., Masterton, S., Stelling, G. S., and J., M. Estimations of infra-

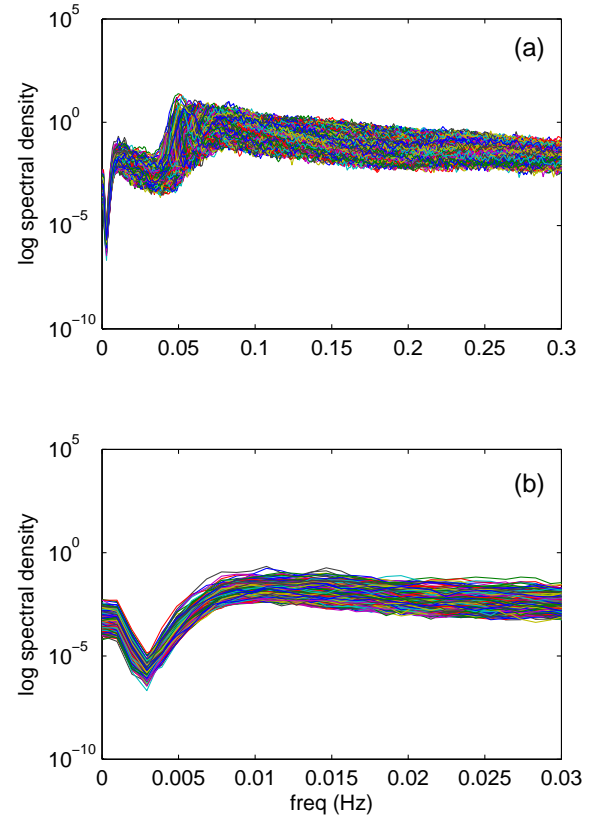


Figure 12: Spectral shape measured at the Baja location: (a) log spectral density including short waves on frequency scale 0–0.3Hz; (b) log spectral density for infragravity frequencies on frequency scale 0–0.03Hz

gravity waves for ship motions. Article in preparation for Coastal Engineering. [4](#), [7](#)